



**One-pot Synthesis of Enzyme@Metal-Organic Materials
(MOM) Biocomposites for Enzyme Biocatalysis**

Journal:	<i>Green Chemistry</i>
Manuscript ID	GC-ART-03-2021-000775.R1
Article Type:	Paper
Date Submitted by the Author:	15-Apr-2021
Complete List of Authors:	Pan, Yanxiong; North Dakota State University, Chemistry and Biochemistry Li, Hui; North Dakota State University, Department of Chemistry and Biochemistry Lenertz, Mary; North Dakota State University Han, Yulun; North Dakota State University, Department of Chemistry and Biochemistry; University of South Dakota, Department of Chemistry Ugrinov, Angel; North Dakota State University, Dept of Chemistry and Biochemistry Kilin, Dmitri; North Dakota State University, Department of Chemistry and Biochemistry Chen, Bingcan; North Dakota State University, Plant Sciences Yang, Zhongyu; North Dakota State University, Chemistry and Biochemistry

One-pot Synthesis of Enzyme@Metal-Organic Materials (MOM)

Biocomposites for Enzyme Biocatalysis

Yanxiong Pan,¹ Hui Li,² Mary Lenertz,¹ Yulun Han,¹ Angel Ugrinov,¹ Dmitri Kilin,¹ Bingcan Chen,^{*,2} and Zhongyu Yang^{*,1}

1. Department of Chemistry and Biochemistry, North Dakota State University, Fargo, ND, 58102
2. Department of Plant Sciences, North Dakota State University, Fargo, ND, 58102

Corresponding to: zhongyu.yang@ndsu.edu; Bingcan.chen@ndsu.edu

Abstract

Metal-Organic Frameworks/Materials (MOFs/MOMs) are advanced enzyme immobilization platforms that improve biocatalysis, materials science, and protein biophysics. A unique way to immobilize enzymes is co-crystallization/co-precipitation, which removes the limitation on enzyme/substrate size. Thus far, most enzyme@MOF composites rely on the use of non-sustainable chemicals and, in certain cases, heavy metals, not only creating concerns on environmental conservation but also limiting their applications in nutrition and biomedicine. Here, we show that a dimeric compound derived from lignin, 5,5'-dehydrodivanillate (DDVA), co-precipitates with enzymes and low-toxicity metals, Ca^{2+} and Zn^{2+} , and forms stable enzyme@Ca/Zn-MOM composites. We demonstrated this strategy on four enzymes with different isoelectric point (IEP), molecular weight, and substrate size. Furthermore, we found all enzymes displayed slightly different but reasonable catalytic efficiencies upon immobilization in the Ca-DDVA and Zn-DDVA MOMs, as well as reasonable reusability in both composites. We then probed the structural basis of such difference using a representative enzyme and found enhanced restriction of enzyme in Zn-DDVA than in Ca-DDVA, which may cause the activity difference. To our best knowledge, this is the first aqueous-phase, one-pot synthesis of lignin-derived “green” enzyme@MOF/MOM platform that can host enzymes without any limitation on enzyme IEP, molecular weight, and substrate size. The different morphology and crystallinity of the composites formed by Ca-DDVA and Zn-DDVA MOMs broaden their applications depending on the problem of interest. Our approach of enzyme immobilization not only improves the sustainability/reusability of almost any enzymes but also reduces/eliminates the use of non-sustainable resources. The synthetic method places negligible environmental impact while the products are non-toxic to living things and the environment. The biocompatibility also

makes it possible to carry out enzyme delivery/release for nutrition or biomedical applications via our “green” biocomposites.

Introduction

Metal-Organic Frameworks (MOFs) are advanced enzyme immobilization platforms offering enhanced enzyme protection, substrate diffusivity/selectivity, and catalytic efficiency, and thus, have improved biocatalysis, energy, materials, and protein biophysics research.¹⁻⁸ Enzyme immobilization on MOFs, thus, has significantly improved the sustainability/reusability of the expensive enzymes, placing a positive impact on green chemistry. Thus far, many enzymes have been proved functional upon encapsulation in MOFs, including those smaller than MOF apertures as well as larger enzymes/enzyme clusters,⁹⁻¹² the latter of which often relies on the co-precipitation of enzymes with metals/ligands. The substrates, on the other hand, are often limited to those smaller than MOF apertures. We recently found that large substrates can also be catalyzed by enzymes via co-precipitation, which removed the size limitation on enzyme and substrate.¹³⁻¹⁶

In spite of the exciting discoveries on co-precipitation-based enzyme immobilization, a number of concerns have been raised. For example, one way to prepare enzyme@MOF (such as the enzyme@Zeolitic-Imidazolate Frameworks, ZIFs) is to co-precipitate the enzyme and metal/imidazolate in the organic phase (ca. MeOH),¹⁷ and the target enzymes have to be protected by a polymer to avoid damage by the solvent. However, this is not ideal for all enzymes. It is also possible to prepare enzyme@MOF co-precipitates in the aqueous-phase (such as the biomineralization of enzymes and Zn²⁺/imidazolate derivatives), which also generate decent crystals.¹⁸⁻²⁰ However, the ligands in these works may chelate the endogenous metal ions (such as Ca²⁺, Cu²⁺, and Zn²⁺) in certain metalloproteins, damaging enzyme function.²¹ Lastly and most importantly, the ligands of most current MOFs are non-renewable chemicals based on petrochemical resources, some of which are not health/environment-friendly and may even

possess toxicity.^{22, 23} This barrier raises concerns/cautions on the environmental impact of the MOFs due to the need of non-renewable petroleum resources as well as when applying the enzyme@MOF composites in food, nutrition, and biomedicine science/industry. Alternative ligands are required.

To overcome these barriers, we are exploring alternative metals and biocompatible ligands for co-precipitation with enzymes. We found a ligand from sustainable natural sources, the lignin-derived, dimeric compound, 5,5' - dehydrodivanillate (DDVA), can co-precipitate enzymes with low-toxicity metals. DDVA is originated from a part of lignin,²⁴ a biomass from plants whose growth only requires sunlight, oxygen, and water. Furthermore, DDVA has been considered as a nutrient for certain bacteria which employ certain enzymes to convert DDVA, indicating the high biocompatibility and low toxicity of DDVA.^{25, 26} The metal centers, Ca²⁺ and Zn²⁺, are also considered as less-toxic metals. Co-precipitating enzymes with Ca/Zn and DDVA resulted in layer-by-layer structures of crystal-like composites. We thus name the resultant composites Ca-/Zn-based MOMs, to distinguish from the 3-dimensional structures of classic MOFs. The resultant enzyme@MOM composites possess all aforementioned advantages such as the ease of operation as well as no size limitation on enzyme and substrate. Interestingly, the enzyme@Ca-DDVA and enzyme@Zn-DDVA MOM-based composites display different morphology and crystallinity. We tested both MOMs on four enzymes with different isoelectric point (IEP), molecular weight, and substrate size, lysozyme (lys, 18.7 kDa; substrate: bacterial cell walls; IEP: 9.2), lipase (53 kDa; substrate: esters; IEP: 5.8), glucose oxidase (GOx, 80 kDa; substrate: glucose; IEP 4.2), and horseradish peroxidase (HRP, 44 kDa; substrate: H₂O₂; IEP: 3-9). We found that all enzymes display the expected catalytic activity in the enzyme@Ca-DDVA and enzyme@Zn-DDVA biocomposites, with a higher catalytic efficiency in the former. In

addition, the loading capacity and reusability of the immobilized enzymes are decent. Lastly, we carried out site-directed spin labeling (SDSL)-Electron Paramagnetic Resonance (EPR) studies^{16, 27-29} to probe the possible structural basis of the relatively high catalytic efficiency on a representative enzyme, and found potential origins of the activity difference.

To our best knowledge, this is the first report on immobilizing enzymes with arbitrary IEP, molecular weight, and substrate size in a biocompatible, lignin-based, “green” MOF/MOM via a simple, aqueous-phase, one-pot “green” synthesis. The ligand is originated from lignin-derivatives which can help reduce the use of non-renewable chemicals and save petroleum sources; the compound can serve as the nutrient of certain bacteria, indicating the high biocompatibility. The synthetic conditions are “green” too which do not require heating, pressure, or organic solvents. These aspects open an avenue for the “green” synthesis of “sustainable”, “green” enzyme@MOM composites. Different from the existing “green” MOF works,³⁰⁻³⁸ for the first time our approach allows for the immobilization of enzymes in the “green” MOMs and demonstrates the biocatalytic activity of the involved enzymes. The decent loading capacity is another advantage. The different morphology and crystallinity of the composites formed by Ca^{2+} and Zn^{2+} make it possible to apply our composites according to the problem of interest. Our approach of enzyme immobilization not only improves the sustainability/reusability of almost any enzymes but also reduces/eliminates the use of non-sustainable resources. The synthetic method places negligible environmental impact while the products are non-toxic to living things and the environment. The biocompatibility and/or biodegradability of metals and DDVA ligand make it possible to carry out enzyme release for nutrition or biomedical applications via our “green” enzyme@MOF/MOM composites.

Result and Discussion

Selection of metal and ligand. We are particularly interested in ligands derived from plants because of their growth only requires sun, soil, and water, and their biocompatibility, high structural variety, and great natural sources. After a careful screening, we found that a dimeric compound derived from lignin, DDVA, can form coordination bonds with some low-toxicity metal ions such as Zn^{2+} and Ca^{2+} (as compared to other metals often encountered in MOF research) via their hydroxyl, carboxyl, and ether groups. Remarkably, DDVA is able to immobilize enzymes during its co-crystallization with Zn^{2+} or Ca^{2+} in a “green” condition, ambient temperature and pressure in the aqueous phase. Thus, this work is focused on the aqueous-phase co-precipitation of DDVA with Zn^{2+} or Ca^{2+} and several enzymes.

Synthesis and characterization of enzyme@Ca-DDVA and Zn-DDVA biocomposites. The reaction schemes to prepare the enzyme@Ca-DDVA or Zn-DDVA in water at room temperature (RT) are shown in **Fig. 1** with details provided in the Electronic Supplementary Information (ESI). The scanning electron microscope (SEM) images shown in **Fig. 2** indicate that both composites are round shaped particles with Ca-DDVA larger in size than Zn-DDVA (**Fig. 2a&d**). The surface of the Ca-DDVA show more regular shapes while that of the Zn-DDVA possesses flower-like porous materials (**Fig. 2b versus 2e**). The incorporation of enzymes in both composites was confirmed via attenuated total reflectance (ATR)-Fourier Transformation Infrared (FTIR) spectroscopy (**Figure S1**), wherein the presence of the 1640 cm^{-1} peak upon enzyme incorporation due to the protein C=O stretching vibration indicates the presence of protein molecules. We have also employed the fluorescein isothiocyanate (FITC) to label each enzyme and incorporated the labeled enzymes into Ca-DDVA and Zn-DDVA. The resultant confocal fluorescent images confirmed the successful inclusion of enzymes (representative data on lys is shown in **Fig. 2c&f**).

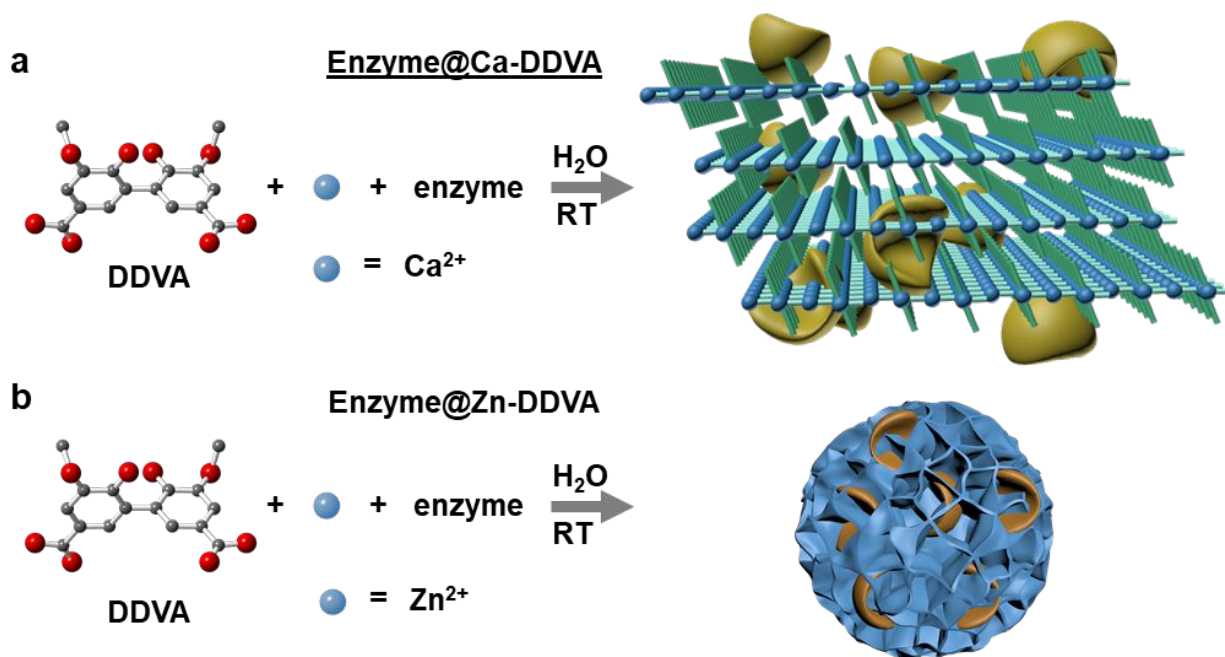


Fig. 1. Reaction schemes of the preparation of the enzyme@Ca-MOM composites. (a) Preparation of the enzyme@Ca-DDVA in water at room temperature (RT). (b) Preparation of the enzyme@Zn-DDVA in water at RT. The morphologies of the resultant composites are derived based on our experimental finding (see Fig. 2). Yellow/orange models represent enzymes in the composites.

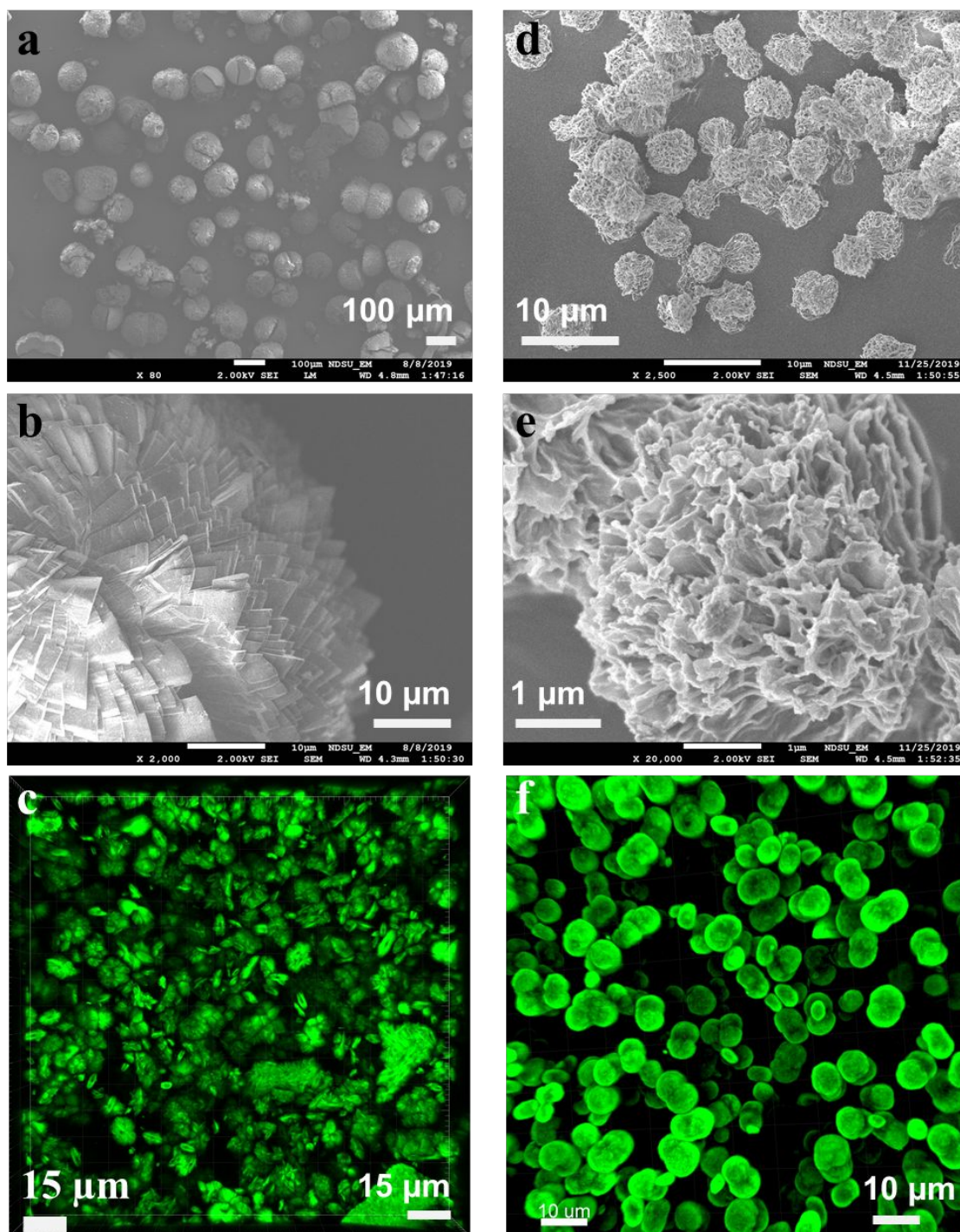


Fig. 2. Images of the enzyme@MOM composites. (a,b) The SEM images of the lys@Ca-DDVA at different length scales. (c) The confocal fluorescent images of FITC-labeled lys in Ca-DDVA. (d, e) The SEM images of the lys@Zn-DDVA at different length scales. (f) The confocal

fluorescent images of FITC-labeled lys Zn-DDVA. (c) and (f) indicate the successful inclusion of the representative enzyme in each composite.

The powder X-ray diffraction (PXRD) patterns of the enzyme@Ca-DDVA are similar to the single-crystal XRD pattern of pure Ca-DDVA prepared under a higher temperature (60 °C; **Fig. 3a**), which indicates a layer-by-layer structure. Within each layer, as shown in **Fig. 4a**, “sub-layers” are also present. A closer look at the crystal structure indicates two categories of Ca²⁺ coordination. First, as shown in **Fig. 4b**, each Ca²⁺ ion is coordinated with an ether and a hydroxyl group from a DDVA above and those from another DDVA below; four water molecules are also coordinated. This category of Ca²⁺ coordination seems to be the driving force connecting the sub-layers. Second, within a sub-layer, two Ca²⁺ in close proximity are stabilized by four DDVAs. Each Ca²⁺ is coordinated with an ether and a hydroxyl group from a DDVA (see OH₁ and ether₁ for the top Ca²⁺ of **Fig. 4c** and OH₄ and ether₄ for the bottom Ca²⁺) and a carboxyl group from another DDVA (see COOH₂ for the top Ca²⁺ of **Fig. 4c** and COOH₃ for the bottom Ca²⁺). The carboxyl groups keep two Ca²⁺ in close proximity. Interestingly, in each DDVA, there is one carboxyl group that does not participate in coordination, which may facilitate enzyme contact and thus, incorporation. The diffraction pattern of Zn-DDVA suggests that only amorphous structure was formed (**Fig. 3b**), consistent with the irregular, porous materials shown by SEM (**Fig. 2e**). The co-crystallization of metals and ligands not only depends on the orbital/charge/size of the metal but also the structure of the ligand, both of which determine how the metal coordinates with the ligand. To form crystals, Zn²⁺ is more preferential to coordinate with imidazoles while Ca²⁺ is commonly seen to coordinate with carboxylates (such as terephthalic acid, also known as BDC).^{19, 39} We observed a relatively rare case that Zn²⁺

coordinates with a carboxylate compound, DDVA, likely caused by the presence and specific arrangement of the multiple carboxylate groups in DDVA (since Zn^{2+} and BDC do not form crystals at room temperature under aqueous conditions). At the current stage, we do not have definitive evidence to conclusively identify the origins of the low crystallinity of the Zn-DDVA in comparison to the Ca-DDVA. We do not have a clear picture of the crystal structure of the Zn-DDVA either. Our judgement of the partial crystalline nature of the Zn-DDVA was solely based on the broadened PXRD pattern. Revealing such a mystery is our on-going work.

The thermal gravimetric analysis (TGA) data of Ca-/Zn-DDVA MOMs in the absence and presence of enzymes indicate the entrapment of enzymes in both composites (representative data see **Fig. 3c&d**). The presence of enzyme does not seem to significantly impact the thermostability of Ca-DDVA and Zn-DDVA alone. The amounts of entrapped enzymes in both composites were determined using the bicinchoninic acid (BCA) assay.⁴⁰ Typically, ~ 10% and ~6.7% (w/w) of enzyme loading capacity were found for enzyme@Ca-DDVA and enzyme@Zn-DDVA, respectively, comparable or slightly higher than those reported in the literature.¹⁰ Only representative data of XRD and TGA using lys@Ca-DDVA or Zn-DDVA are shown here. Other enzymes display similar trends/patterns and are not shown for conciseness of the paper.

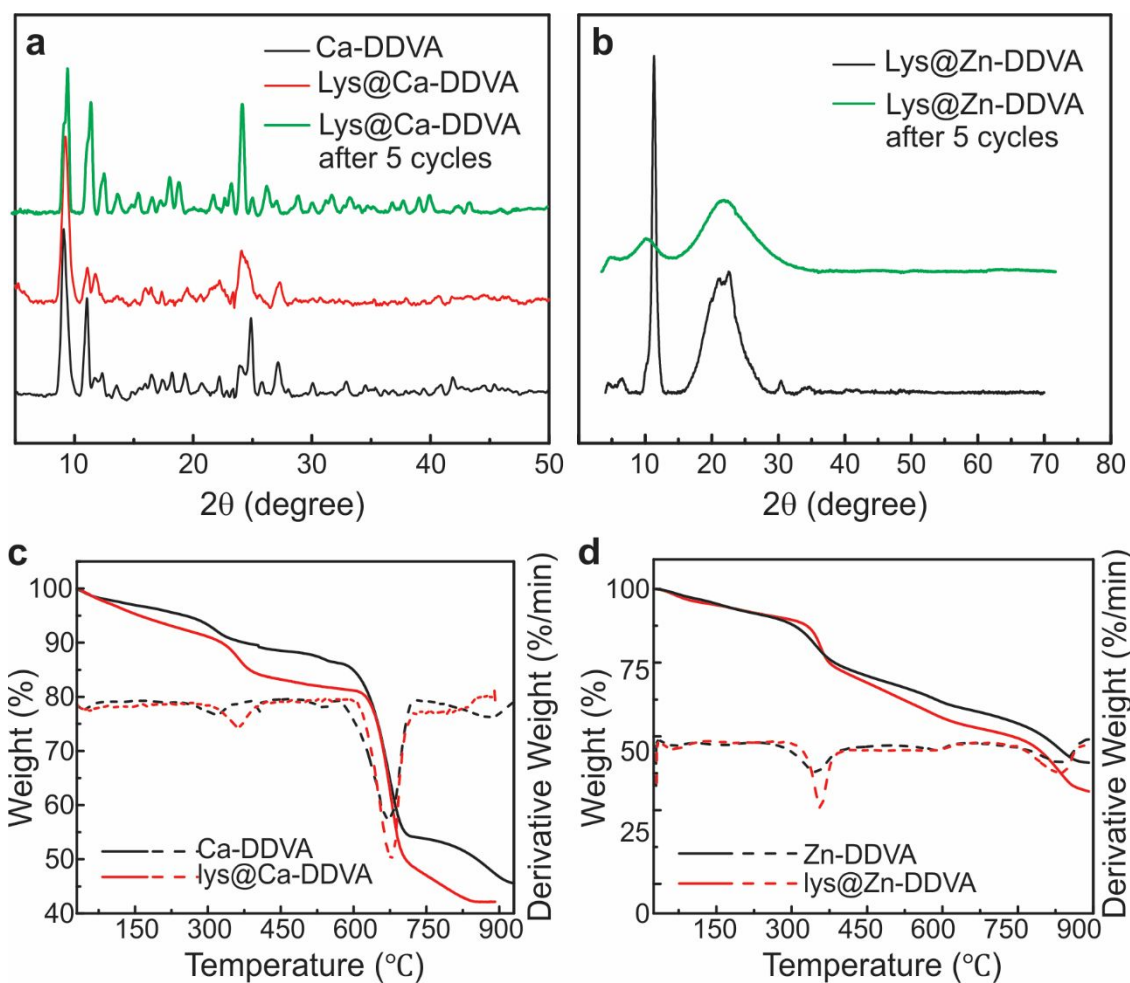


Fig. 3. Characterization of the enzyme@Ca-/Zn-MOM composites. (a) The XRD data of the lys@Ca-DDVA composites developed in this work before and after 5 catalytic cycles (green). (b) The PXRD of lys@Zn-DDVA before and after 5 catalytic cycles (green). (c) The TGA data of lys@Ca-DDVA as representatives of enzyme@MOM platforms suggested the inclusion of enzyme into the composites. (d) The TGA data of lys@Zn-DDVA.

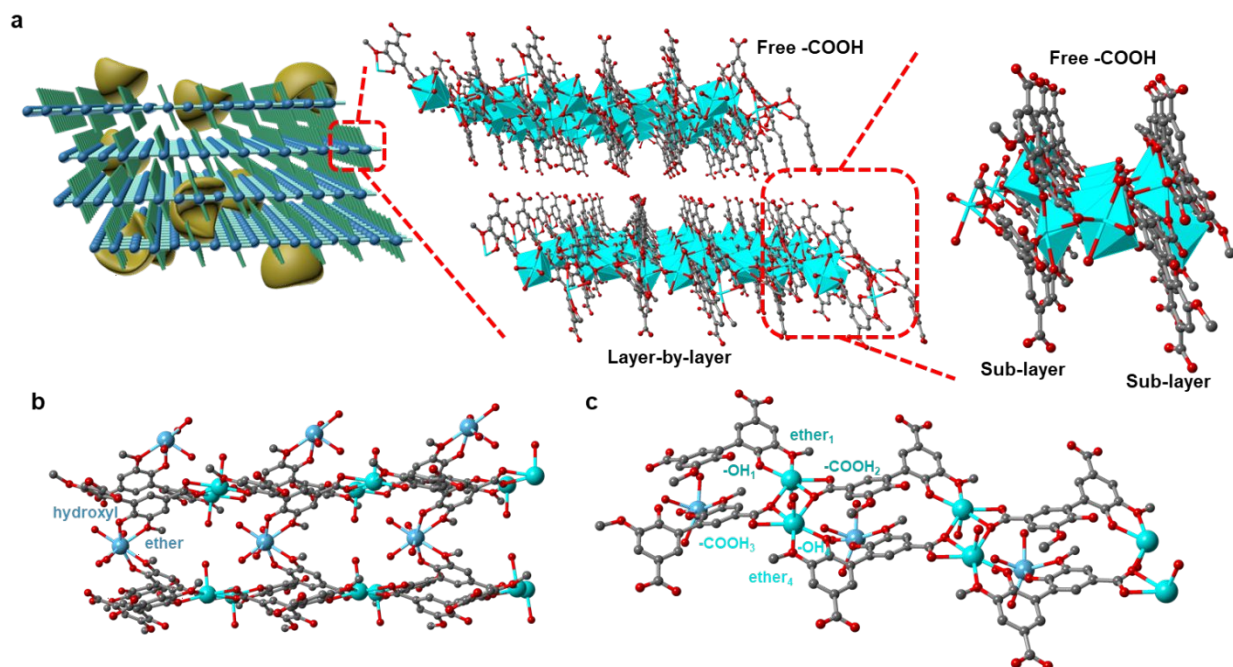


Fig. 4. Structure of the Ca-DDVA. (a) The structure of the single-crystal Ca-DDVA at different length scales. (b) The first Ca^{2+} coordination: each Ca^{2+} in between the sub-layers are coordinated with an ether and a hydroxyl group. (c) The second Ca^{2+} coordination: two Ca^{2+} in close proximity. Each Ca^{2+} in the same sub-layer are coordinated with an ether and a hydroxyl group from one DDVA (see subscripts 1 and 4) and a carboxyl group from an adjacent DDVA (see subscripts 2 and 3). The carboxyl groups keep two Ca^{2+} in close proximity. In each DDVA, there is one carboxyl group that does not participate in coordination.

Catalytic activity of enzymes on both composites. To generalize our platform for enzyme incorporation, we employed four enzymes that are commonly studied as models in biocatalysis, lys, lipase, GOx, and HRP. Each enzyme was hosted in Ca-DDVA and Zn-DDVA, respectively (characterization see above). The catalytic activity of each enzyme in each MOM-based composite was then investigated using the corresponding activity assays.

The physiological substrate of lys is the bacterial cell walls.⁴¹ To quantify lys activity, the commercial activity kit, EnzChek® Lysozyme Assay Kit (see the ESI) was employed, which monitors the generation of fluorescence signal using the fluorescein labeled *Micrococcus lysodeikticus* cell walls as substrates. As controls, the product generation as a function of free lys concentration is close to be linear (**Figure S5**), while the DDVA alone, Ca-DDVA (no lys), and Zn-DDVA (no lys) did not generate any product (**Figure S6**). The catalytic activity of free lys, lys@Ca-DDVA, and lys@Zn-DDVA under the same enzyme loading amount (determined by the BCA assay) is shown in **Fig. 5a&b**. Both composites show reduced catalytic efficiency against the same substrate as compared to the free lys, reasonable given the reduced mobility of composites and the partial exposure of the lys enzyme on the composite surface (structural basis see below). Lys@Zn-DDVA displays a lower catalytic efficiency than lys@Ca-DDVA, likely because of the rugged surface of the Zn-DDVA composites as compared to the smooth and large surface of the Ca-DDVA (see SEM images of **Fig. 2**), which may prevent effective contact with the large substrate. The enzymatic kinetics parameters, V_{max} and K_m , were calculated under increasing substrate concentrations and summarized in Table 1, which confirmed the relative catalytic efficiency discussed above. Error bars were obtained via three repeated measurements under the same condition (substrate concentration, buffer pH, etc).

Table 1. The kinetic parameters of the hydrolysis of *Micrococcus lysodeikticus* cell walls catalysed by free lys and the lys@Ca-DDVA/Zn-DDVA composites obtained via the Michaelis-Menten method.

Parameters	V_{max} (U/min)	K_m (U)	R^2
lys	316.4±194.5	308.3±222.0	0.9889
lys@Ca-DDVA	136.3±44.1	175.8±73.4	0.9910

lys@Zn-DDVA	18.1±2.8	64.8±16.9	0.9883
-------------	----------	-----------	--------

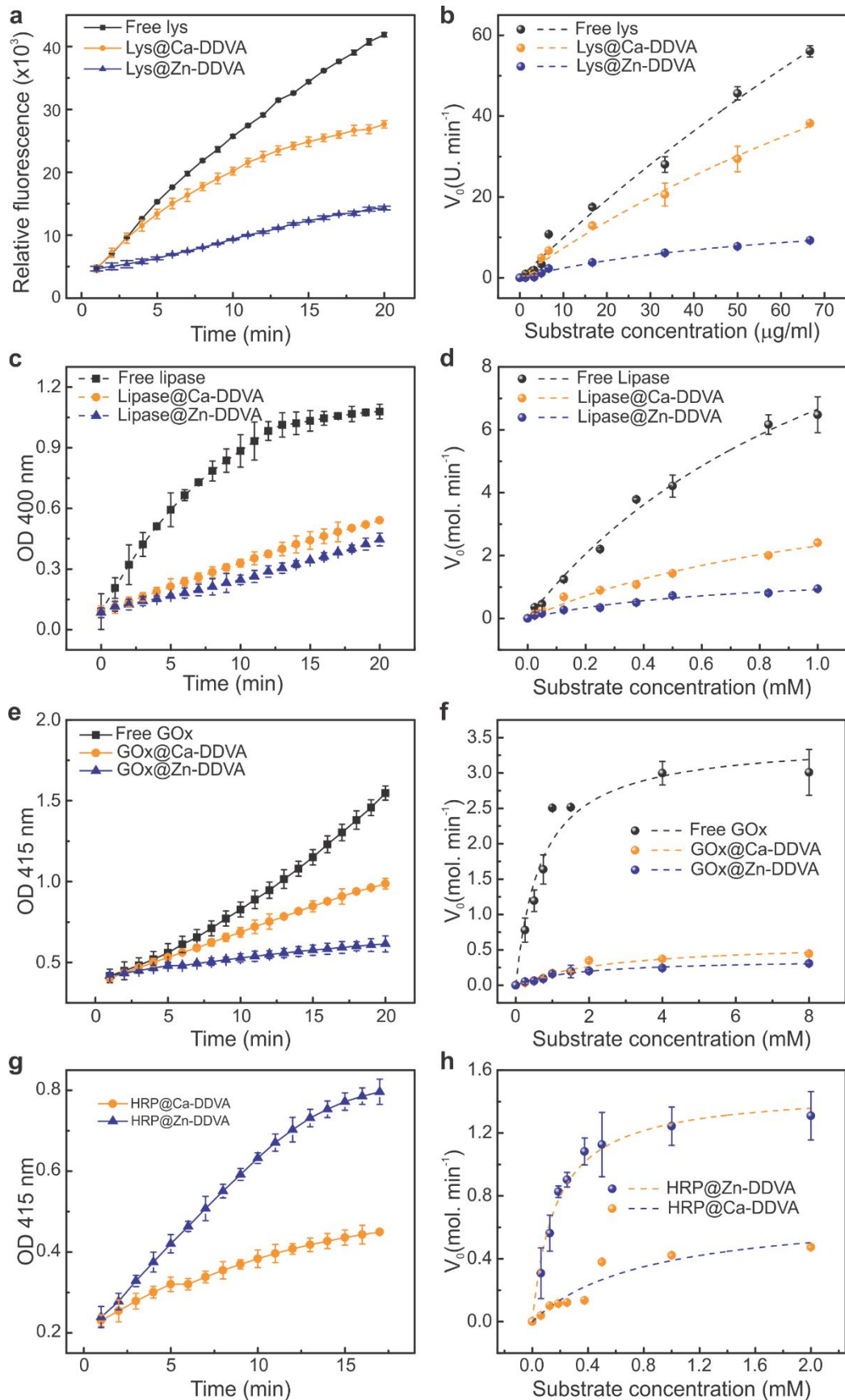


Fig. 5. Activity assays of each enzyme@MOM composites. (a,c,e,g) Representative data of the catalytic activity assays of lys (a), lipase (c), GOx (e), and HRP (g) upon loading into each composite. (b,d,f,h) The enzymatic kinetics analysis with fitting of each enzyme. Data analysis and fitting see the main text and the ESI.

The lipase catalytic activity was assessed by quantifying the generation of acetic acid and 4-nitrophenol when 4-nitrophenyl acetate is hydrolyzed by lipase. Here the 4-nitrophenol has a UV-vis absorption at 400 nm which was monitored over time.⁴² Upon confirming DDVA alone, Ca-DDVA (no lipase), and Zn-DDVA (no lipase) did not generate any 4-nitrophenol (**Figure S7**), under the same enzyme amount, free lipase, lipase@Ca-DDVA, and lipase@Zn-DDVA composites show the formation of 4-nitrophenol (**Fig. 5c**). Free lipase shows much higher catalytic efficiency as compared to the composites, likely due to the reduced substrate diffusion within our MOM network. Lipase@Ca-DDVA shows slightly higher efficiency than lipase@Zn-DDVA. The V_{max} and K_m calculations (**Fig. 5d**, right and Table 2) also indicate the same trend.

Table 2. The kinetic parameters of free lipase and the synthesized lipase@Ca-DDVA/Zn-DDVA composites.

Parameters	V_{max} ($\mu\text{mol}/\text{min}$)	K_m (μM)	R^2
lipase	37.0 \pm 4.7	0.97 \pm 0.21	0.989
lipase@Ca-DDVA	9.7 \pm 1.3	0.94 \pm 0.21	0.988
lipase@Zn-DDVA	5.2 \pm 0.4	0.56 \pm 0.94	0.989

HRP is needed for GOx activity assessment as described in the literature.^{9, 43} In detail, GOx degrades glucose and generate glucono-lactone and H_2O_2 ; HRP was then added together with the

produced H_2O_2 to convert the 2,2'-Azino-bis(3-ethylbenzothiazoline-6-sulfonic acid) diammonium salt (ABTS) to $\text{ABTS}^{+\bullet}$. The latter displays a UV-vis absorption at 415 nm, which was monitored over time.^{44, 45} With HRP, upon confirming DDVA, Ca-DDVA (no lipase), and Zn-DDVA (no lipase) did not generate $\text{ABTS}^{+\bullet}$, under the same GOx amount, free GOx and the two composites show the formation of $\text{ABTS}^{+\bullet}$ (**Fig. 5e**), although the efficiency is much lower in the composites than free GOx, likely due to the reduced enzyme mobility and substrate diffusivity. GOx@Ca-DDVA stills shows slightly higher efficiency than GOx@Zn-DDVA. The V_{max} and K_m calculations (**Fig. 5f** and Table 3) also indicate the same trend.

Table 3. The kinetic parameters of the GOx@Ca-DDVA/Zn-DDVA and HRP@Ca-DDVA/Zn-DDVA composites.

Parameters	V_{max} (mmol min ⁻¹ mg ⁻¹)	K_m (mM)	R^2
GOx@Ca-DDVA	0.62 ± 0.09	2.69±0.81	0.939
GOx@Zn-DDVA	0.37±0.03	1.76±0.35	0.964
HRP@Ca-DDVA	0.71±0.15	0.83±0.36	0.972
HRP@Zn-DDVA	1.47±0.08	0.17±0.2	0.969

HRP activity was studied similarly except that H_2O_2 was provided to free HRP and HRP@Ca-DDVA and HRP@Zn-DDVA composites (**Fig. 5g**). Different from above trends, HRP@Zn-DDVA shows slightly higher efficiency than HRP@Ca-DDVA (**Fig. 5h** and Table 3). Lastly, both Ca-DDVA and Zn-DDVA are able to encapsulate both GOx and HRP and carry out cascade biocatalysis. Representative data set is shown in the ESI (**Figure S8**).

Reusability and stability of the composites.

The reusability of the Ca-DDVA and Zn-DDVA was assessed using lipase as the representative enzyme. We chose lipase because of the convenience of testing lipase activity, which requires less time and materials/resources. The V_{max} after up to 5 reuse cycles was calculated as described above and plotted as the relative activity in % in **Fig. 6**. Both composites show more than 80% reusability for lipase, with lipase@Zn-DDVA displaying a higher relative activity than lipase@Ca-DDVA. The composites are stable after these five repeated cycles as shown in the PXRD data before and after reuses (Figure 3a&b green). The amorphous Zn-DDVA seemed to lose some more crystallinity as indicated by the broadened peaks. However, the particles were present the whole time, enabling their high reusability. The drop in the relative activity (Figure 6) is likely caused by a combination of enzyme function loss (due to multiple cycles) as well as the enzyme quantity loss (due to sample loss). To quantify the enzyme loss between washes, we prepared a series of identical aliquot samples and performed the reusability test in parallel. After each cycle, we disassembled one aliquot and measured the entrapped enzyme. We found the enzyme loss is small (less ~ 1% loss), which can be considered negligible when evaluating the reusability and V_{max} .

Enzyme immobilization using MOMs based on Ca-DDVA and Zn-DDVA improved the stability of the enzyme. In particular, as shown in Figure S10, the relative activity of lipase after storage on bench for 7 days is comparable to that of the lipase@Ca-DDVA. Interestingly, the lipase@Zn-DDVA seemed to show a better stability than the Ca-DDVA and free enzyme, in line with the better reusability of lipase@Zn-DDVA. In pure water under 4 °C, the composites are stable for at least 2 weeks. Weakly basic pHs are required when using our composites for biocatalytic reactions. In fact, most enzymes (especially the four representatives discussed in this work) can have reasonable catalytic performance, indicating our platform can be applicable to

many enzymes. We are continuously discovering other green ligands to form acid-stable composites that can immobilize enzymes.

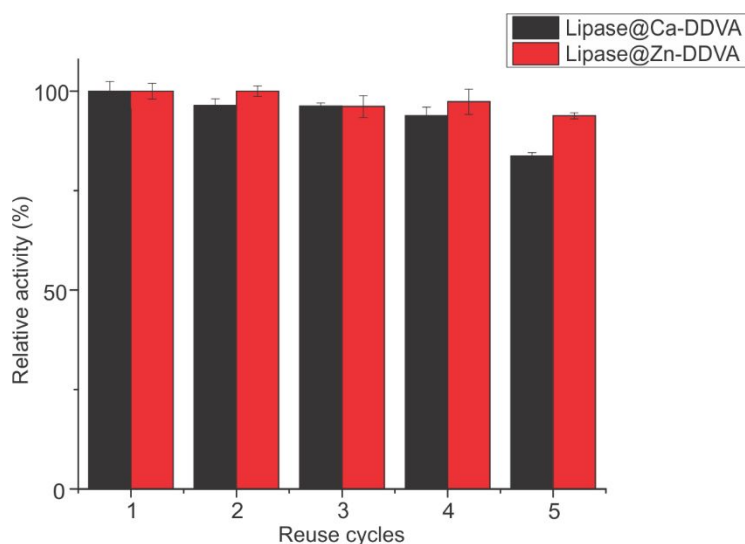


Fig. 6. The relative reusability of the Ca-/Zn-DDVA MOF composites when lipase is studied as the model enzyme. Within 5 cycles, both composites show \sim 80% relative catalytic efficiency. Lipase@Zn-DDVA shows higher reusability than lipase@Ca-DDVA.

Structural basis of large substrate biocatalysis. Similar to our recent finding,¹⁶ we propose that the partial exposure of lys encapsulated in the MOM-based composite is the cause of enzyme contact with large-size substrate. Here we employ the similar principles developed in our recent work¹⁶ to determine the chance of exposing different lys regions above the surface of each of the DDVA-based MOMs developed in this work. In brief, we site-specifically labeled (**Fig. 7a&b**) a model enzyme, lys, and determined the backbone dynamics of multiple labeled sites on lys using Electron Paramagnetic Resonance (EPR) spectroscopy (**Fig. 7c&d**). This approach is immune of the complexities caused by the MOF/MOM backgrounds and is sensitive to ns-scale protein sidechain motion.¹⁸ In addition, a labeled protein residue exposed above the MOF/MOM crystal to the reaction medium would display enhanced dynamics (often designated as the “m”

component which stands for mobile) as compared to those buried inside of the MOF/MOM (“im” component stands for immobile; see **Fig. 7c-f**). The relative population of each case can be determined via spectral simulation if both cases exist for the same labeled residue (**Fig. 7e&f**).¹⁶

46-48

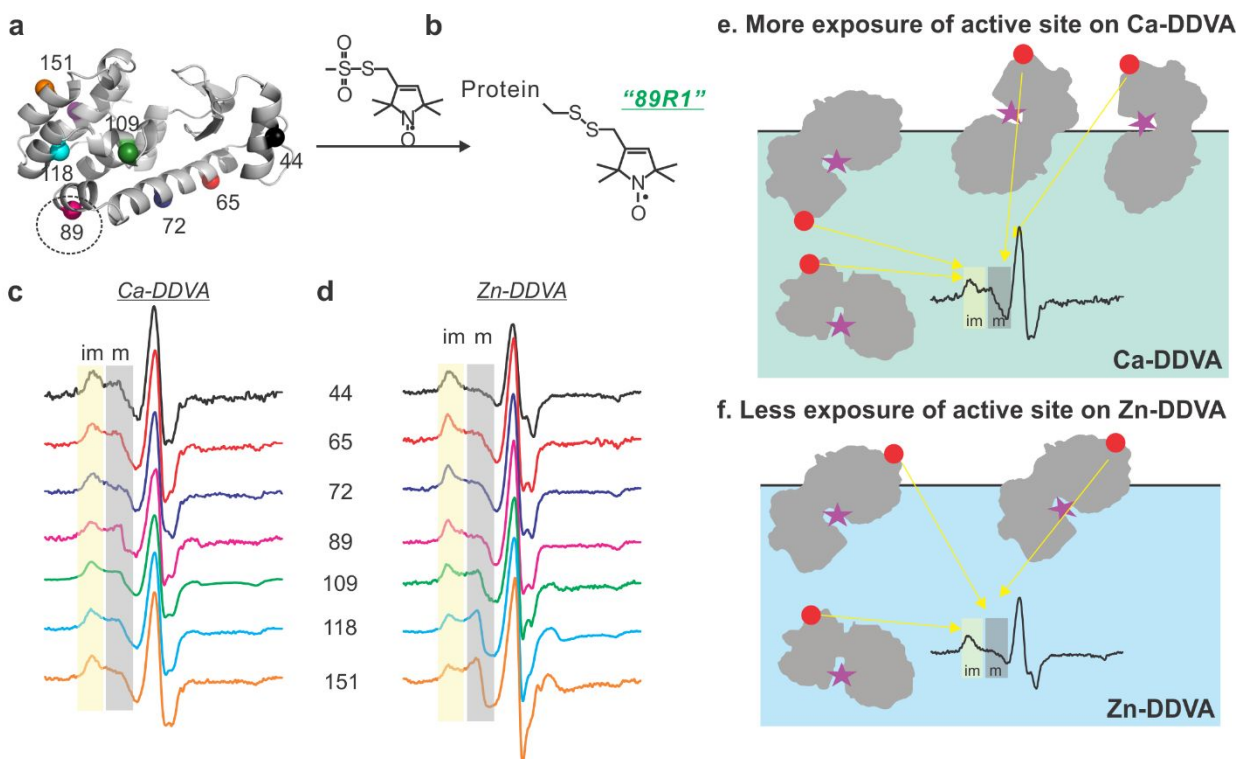


Fig. 7. Probing the structural basis of the catalytic behavior using lys@MOM as a model system. (a) The surface residues that are spin labeled with a nitroxide (b) for structural study. (c, d) The EPR spectrum of each labeled mutant upon encapsulation to each DDVA-based composites. (e, f) Schematic illustration of the exposable region of lys on Ca-DDVA and Zn-DDVA surface as determined via EPR. Star=lys active site.

In detail, as shown in **Fig. 7c&d**, although both “m” and “im” components are observed for each mutant, there is a significant increase in the “m” component (due to exposure above the crystal surface) in Ca-DDVA in the N-terminus and near the active site (see the high “m” peak intensity

for 44 and 65) as compared to the “m” component intensity in Zn-DDVA at the same region. In contrast, in Zn-DDVA, the C-terminus of lys shows enhanced chance of exposure (see the high “m” peak intensity for 109, 118, and 151). Because the C-terminus is further away from the active site, our structural study indicates that there is a high chance for lys to display lower catalytic efficiency in Zn-DDVA due to the less chance of active site exposure to the reaction medium (and contact the large substrate; **Fig. 7F**). Spectral simulations detailed in the ESI also confirmed the same conclusion, wherein the N-terminal residues of lys in Ca-DDVA show a higher “m” component population (47.5% and 58.5% for residues 44 and 65) than that in Zn-DDVA (28.0% and 49.2% for residues 44 and 65), indicating a higher chance of the N-terminus being exposed in the former. Interestingly, for the “im” component which was caused by the enzyme buried under the MOM surface, the ordering parameters (see C_{20} and C_{22} of Table S3&S4) indicate a higher degree of restriction in the sidechain motion of the labeled sites in Zn-DDVA as compared to those in Ca-DDVA. Also, the rate parameters (see $R_{z,im}$ of Table S3&S4) suggest a reduced motion of the sidechain motion of the labeled sites in Zn-DDVA as compared to those in Ca-DDVA. These together leads to a speculation that most enzymes (3 out of 4, in our study) may encounter more restriction in Zn-DDVA, which results in the reduced catalytic efficiency.

Discussions

The different properties of the Ca- and Zn-DDVA composites make it possible to apply our composites depending on the problem of interest. For example, if the target system can tolerate one metal over the other, then one can choose the composite based on such a need. In addition, although the catalytic efficiency of enzyme@Ca-DDVA seems to be better than that of enzyme@Zn-DDVA in 3 out of the 4 studied enzymes, a unique advantage of the enzyme@Zn-

DDVA composites is that they can diffuse into smaller gaps and/or make more efficient contact with large, rigid substrates (such as those frequently encountered in food research). It is also promising to use the enzyme@Zn-DDVA composites for penetrating certain biological barriers for biomedical applications. Lastly, lipase@Zn-DDVA displayed a higher reusability as compared to lipase@Ca-DDVA, indicating the possibility that enzyme@Zn-DDVA can be reused for more catalytic cycles. Thus, the enzyme@Zn-DDVA composites are also useful and worth developing/investigating.

Although proved only a minor drawback by various experiments via different approaches, the cytotoxicity of MOF materials always raises concerns in nutrition and/or medical applications.⁴⁹⁻⁵³ The high biocompatibility and biodegradability of the DDVA ligand and the low toxicity of Ca^{2+} and Zn^{2+} metal ion will likely overcome, or, at least, reduce these concerns. Furthermore, under certain conditions, the loaded enzymes in our platforms may be released by disassembling the MOF/MOM scaffolds, making it possible to deliver enzyme to the desired locations. This effort will broaden the application of our composites to food, nutrition, and health.

Due to the complex coordination manner between Ca^{2+} and DDVA, it is highly possible that such stringent coordination condition (stoichiometry and relative arrangement of ions and ligand molecules in 3D space) cannot be met in metalloproteins. This indicates that our platform may be used to encapsulate metalloproteins containing Ca^{2+} , Cu^{2+} , or Zn^{2+} , further generalizing our method to more enzymes.

The difference in the catalytic efficiencies of the studied enzyme on Ca-DDVA and Zn-DDVA is not so clear at this moment. We suspect that the catalytic efficiency depends on many complex factors such as the substrate diffusion efficiency, the collision efficiency between the enzyme and the substrate, and even the dynamics of the encapsulated enzymes in each MOF.

These factors can further depend on the surface properties, size, and even shape of the composites. For lys, a large-substrate enzyme, we utilized the SDSL-EPR approach to probe the possible explanation. However, more work is needed to understand the structural basis of the performance of the other three enzymes, which is our on-going research direction.

Experimental

Materials and measurements. All chemicals and biochemical supplies were purchased from commercially resources in high purity; the involved experiments were carried out without purification. All characterization, including Powder X-ray diffraction (PXRD), Single-crystal X-ray diffraction (XRD), scanning electron microscopy (SEM), thermal gravimetric analysis (TGA), and FTIR spectroscopy of the involved materials follows the published procedures using equipment described in our recent work.²⁹ The expression, purification, and spin labeling of involved lysozyme mutants follow the procedures described in our recent work.¹⁶ For EPR measurements, each protein mutant was transferred into a borosilicate capillary tube (0.70 mm i.d./1.00 mm o.d.; Wilmad Labglass, Inc.) immediately after mixing the channel-materials. Data were acquired using a Varian E-109 spectrometer equipped with a cavity resonator. All continuous wave (CW) EPR spectra were obtained with an observe power of 200 mW, a modulation frequency of 100 kHz, and a modulation amplitude of 1.0 G.

Conclusions

We discovered that a biocompatible ligand, DDVA, from sustainable natural sources can co-precipitate with enzyme and Ca^{2+} or Zn^{2+} in the aqueous phase at room temperature. This ligand can be derived from the renewable biomass, lignin, whose growth only requires the sun, oxygen, and water while the low toxicity of Ca^{2+} and Zn^{2+} make the resultant MOM a “green” enzyme@MOM composites. We demonstrated this platform on four enzymes with different IEP, molecular weight, and substrate size, all of which showed the expected catalytic performance.

Both composites display decent enzyme loading capacities and reusability. To our best knowledge, this is the first one-pot “green” synthesis of a biocompatible, “green” enzyme@MOM composites that can be originated from sustainable resources and generalized to encapsulate most enzymes with no limitation on IEP, molecular weight, and/or substrate size. The different morphology and crystallinity of the composites formed by Ca^{2+} and Zn^{2+} make it possible to apply our composites depending on the problem of interest. Our approach improves the sustainability/reusability of almost any enzymes as well as reduces/eliminates the use of non-sustainable resources while placing negligible environmental impact. The products are non-toxic to living things and the environment. The biocompatibility and/or biodegradability of metals and DDVA ligand makes it possible to carry out enzyme release for nutrition or biomedical applications via our enzyme@MOF composites.

Author Contribution: B. C., and Z. Y. conceived and designed the research. Y. P., H. L., and M. L. performed the synthesis and catalytic assays. Y. P. and H. L. acquired the EPR data and carried out the data analysis. Y. H., A. U. and D. K. assisted in all data analysis and interpretation. All authors participated in drafting the manuscript and gave approval to the final version.

Conflict of interest. The authors claim no conflict of interest.

Acknowledgements. This work is supported by NSF (#1942596 to Z.Y.) and NDSU New Faculty Startup Funds as well as USDA-NIFA Grant 2021-67021-34002 (to B.C.). We appreciate Prof. Hubbell for generously providing the EPR spectral simulation package.

Notes and references

1. X. Lian, Y. Fang, E. Joseph, Q. Wang, J. Li, S. Banerjee, C. Lollar, X. Wang and H.-C. Zhou, *Chem. Soc. Rev.*, 2017, **46**, 3386-3401.
2. A. Kirchon, L. Feng, H. F. Drake, E. A. Joseph and H.-C. Zhou, *Chem. Soc. Rev.*, 2018, **47**, 8611-8638.

3. X. Wang, P. C. Lan and S. Ma, *ACS Centr. Sci.*, 2020, DOI: 10.1021/acscentsci.0c00687.
4. M. B. Majewski, A. J. Howarth, P. Li, M. R. Wasielewski, J. T. Hupp and O. K. Farha, *CrystEngComm*, 2017, **19**, 4082-4091.
5. P. Li, Q. Chen, T. C. Wang, N. A. Vermeulen, B. L. Mehdi, A. Dohnalkova, N. D. Browning, D. Shen, R. Anderson, D. A. Gómez-Gualdrón, F. M. Cetin, J. Jagiello, A. M. Asiri, J. F. Stoddart and O. K. Farha, *Chem*, 2018, **4**, 1022-1034.
6. R. J. Drout, L. Robison and O. K. Farha, *Coord. Chem. Rev.*, 2019, **381**, 151-160.
7. E. Gkaniatsou, C. m. Sicard, R. m. Ricoux, J.-P. Mahy, N. Steunou and C. Serre, *Mater. Horiz.*, 2017, **4**, 55-63.
8. A. J. Howarth, Y. Liu, P. Li, Z. Li, T. C. Wang, J. T. Hupp and O. K. Farha, *Nat. Rev. Materials*, 2016, **1**, 15018.
9. W.-H. Chen, M. Vázquez-González, A. Zoabi, R. Abu-Reziq and I. Willner, *Nat. Catal.*, 2018, **1**, 689-695.
10. F. K. Shieh, S. C. Wang, C. I. Yen, C. C. Wu, S. Dutta, L. Y. Chou, J. V. Morabito, P. Hu, M. H. Hsu, K. C. W. Wu and C. K. Tsung, *J. Am. Chem. Soc.*, 2015, **137**, 4276-4279.
11. G. Chen, X. Kou, S. Huang, L. Tong, Y. Shen, W. Zhu, F. Zhu and G. Ouyang, *Angew. Chem. Int. Ed.*, 2020, **59**, 2867-2874.
12. Y. Li, P. Zhao, T. Gong, H. Wang, X. Jiang, H. Cheng, Y. Liu, Y. Wu and W. Bu, *Angew. Chem. Int. Ed.*, 2020, **132**, 22726-22732.
13. J. Farmakes, I. Schuster, A. Overby, L. Alhalhooly, M. Lenertz, Q. Li, A. Ugrinov, Y. Choi, Y. Pan and Z. Yang, *ACS Appl. Mater. Interfaces*, 2020, **12**, 23119-23126.
14. S. Neupane, K. Patnode, H. Li, K. Baryeh, G. Liu, J. Hu, B. Chen, Y. Pan and Z. Yang, *ACS Appl. Mater. Interfaces*, 2019, **11**, 12133-12141.
15. Q. Li, Y. Pan, H. Li, L. Alhalhooly, Y. Li, B. Chen, Y. Choi and Z. Yang, *ACS Appl. Mater. Interfaces*, 2020, **In press**.
16. Y. Pan, H. Li, J. Farmakes, F. Xiao, B. Chen, S. Ma and Z. Yang, *J. Am. Chem. Soc.*, 2018, **140**, 16032-16036.
17. F. Lyu, Y. Zhang, R. N. Zare, J. Ge and Z. Liu, *Nano Lett.*, 2014, **14**, 5761-5765.
18. H. An, J. Song, T. Wang, N. Xiao, Z. Zhang, P. Cheng, H. Huang, S. Ma and Y. Chen, *Angew. Chem. Int. Ed.*, 2020, **59**, 16764-16769.
19. Y. Pan, Q. Li, H. Li, J. Farmakes, A. Ugrinov, X. Zhu, Z. Lai, B. Chen and Z. Yang, *Chem Catal.*, 2021, **In press**.
20. K. Liang, R. Ricco, C. M. Doherty, M. J. Styles, S. Bell, N. Kirby, S. Mudie, D. Haylock, A. J. Hill, C. J. Doonan and P. Falcaro, *Nat. Commun.*, 2015, **6**, 7240.
21. R. H. Holm, P. Kennepohl and E. I. Solomon, *Chem. Rev.*, 1996, **96**, 2239-2314.
22. R. S. Forgan, *Encyclopedia of Inorganic and Bioinorganic Chemistry*, 2014, DOI: <https://doi.org/10.1002/9781119951438.eibc2192>, 1-13.
23. I. Imaz, M. Rubio-Martínez, J. An, I. Solé-Font, N. Rosi and D. Maspoch, *Chem. Commun.*, 2011, **47**, 7287-7302.
24. N. Kamimura, S. Sakamoto, N. Mitsuda, E. Masai and S. Kajita, *Curr. Opin. Biotechnol.*, 2019, **56**, 179-186.
25. X. Peng, E. Masai, Y. Katayama and M. Fukuda, *Appl. environ. microbiol.*, 1999, **65**, 2789.
26. T. Sonoki, T. Obi, S. Kubota, M. Higashi, E. Masai and Y. Katayama, *Appl. environ. microbiol.*, 2000, **66**, 2125.

27. W. L. Hubbell, C. J. López, C. Altenbach and Z. Yang, *Curr. Opin. Struct. Biol.*, 2013, **23**, 725-733.
28. C. Altenbach, C. J. López, K. Hideg, W. L. Hubbell, Z. Q. Peter and W. Kurt, in *Methods in Enzymology*, Academic Press, 2015, vol. Volume 564, pp. 59-100.
29. Q. Sun, Y. Pan, X. Wang, H. Li, J. Farmakes, B. Aguila, Z. Yang and S. Ma, *Chem*, 2019, **5**, 3184-3195.
30. S. Kumar, S. Jain, M. Nehra, N. Dilbaghi, G. Marrazza and K.-H. Kim, *Coord. Chem. Rev.*, 2020, **420**, 213407.
31. S. Bao, J. Li, B. Guan, M. Jia, O. Terasaki and J. Yu, *Matter*, 2020, **3**, 498-508.
32. L. Xu, C.-Y. Xing, D. Ke, L. Chen, Z.-J. Qiu, S.-L. Zeng, B.-J. Li and S. Zhang, *ACS Appl. Mater. Interfaces*, 2020, **12**, 3032-3041.
33. J. J. Gassensmith, H. Furukawa, R. A. Smaldone, R. S. Forgan, Y. Y. Botros, O. M. Yaghi and J. F. Stoddart, *J. Am. Chem. Soc.*, 2011, **133**, 15312-15315.
34. J. Yang, C. A. Trickett, S. B. Alahmadi, A. S. Alshammari and O. M. Yaghi, *J. Am. Chem. Soc.*, 2017, **139**, 8118-8121.
35. D. Wu, J. J. Gassensmith, D. Gouvêa, S. Ushakov, J. F. Stoddart and A. Navrotsky, *J. Am. Chem. Soc.*, 2013, **135**, 6790-6793.
36. K. J. Hartlieb, J. M. Holcroft, P. Z. Moghadam, N. A. Vermeulen, M. M. Algaradah, M. S. Nassar, Y. Y. Botros, R. Q. Snurr and J. F. Stoddart, *J. Am. Chem. Soc.*, 2016, **138**, 2292-2301.
37. H. Reinsch, *Euro. J. Inorg. Chem.*, 2016, **2016**, 4290-4299.
38. Y. Feng, Y. Bi, W. Zhao and T. Zhang, *J. Mater. Chem. A*, 2016, **4**, 7596-7600.
39. K. Sumida, M. Hu, S. Furukawa and S. Kitagawa, *Inorg. Chem.*, 2016, **55**, 3700-3705.
40. P. K. Smith, R. I. Krohn, G. T. Hermanson, A. K. Mallia, F. H. Gartner, M. D. Provenzano, E. K. Fujimoto, N. M. Goeke, B. J. Olson and D. C. Klenk, *Anal. Biochemistry*, 1985, **150**, 76-85.
41. D. J. Vocadlo, G. J. Davies, R. Laine and S. G. Withers, *Nature*, 2001, **412**, 835-838.
42. K. Nie, Q. An and Y. Zhang, *Nanoscale*, 2016, **8**, 8791-8797.
43. Y. Zhang, S. Tsitkov and H. Hess, *Nat. Commun.*, 2016, **7**, Article number 13982.
44. Y. Zhang and H. Hess, *Anal. Chem.*, 2020, **92**, 1502-1510.
45. Y. Xiong, J. Huang, S.-T. Wang, S. Zafar and O. Gang, *ACS Nano*, 2020, **in press**.
46. B. J. Bennion and V. Daggett, *Proc. Natl. Acad. Sci.*, 2003, **100**, 5142.
47. F. S. Liao, W. S. Lo, Y. S. Hsu, C. C. Wu, S. C. Wang, F. K. Shieh, J. V. Morabito, L. Y. Chou, K. C. W. Wu and C. K. Tsung, *J. Am. Chem. Soc.*, 2017, **139**, 6530-6533.
48. D. E. Budil, S. Lee, S. Saxena and J. H. Freed, *J. Magn. Reson. A*, 1996, **120**, 155-189.
49. A. Ma, Z. Luo, C. Gu, B. Li and J. Liu, *Inorg. Chem. Commun.*, 2017, **77**, 68-71.
50. C. Tamames-Tabar, D. Cunha, E. Imbuluzqueta, F. Ragon, C. Serre, M. J. Blanco-Prieto and P. Horcajada, *J. Mater. Chem. B*, 2014, **2**, 262-271.
51. I. Abánades Lázaro, C. J. R. Wells and R. S. Forgan, *Angew. Chem. Int. Ed.*, 2020, **59**, 5211-5217.
52. E. S. Grape, J. G. Flores, T. Hidalgo, E. Martínez-Ahumada, A. Gutiérrez-Alejandre, A. Hautier, D. R. Williams, M. O'Keeffe, L. Öhrström, T. Willhammar, P. Horcajada, I. A. Ibarra and A. K. Inge, *J. Am. Chem. Soc.*, 2020, **142**, 16795-16804.
53. S. Wang, Y. Chen, S. Wang, P. Li, C. A. Mirkin and O. K. Farha, *J. Am. Chem. Soc.*, 2019, **141**, 2215-2219.